CRYSTAL GROWTH & DESIGN

Article

pubs.acs.org/crystal

A Series of Multi-Dimensional Lanthanide-Containing Peroxoisopolymolybdates

Jingjing Wei, Lu Yang, Pengtao Ma, Jingping Wang,* and Jingyang Niu*

Henan Key Laboratory of Polyoxometalate Chemistry, Institute of Molecular and Crystal Engineering, College of Chemistry and Chemical Engineering, Henan University, Kaifeng, Henan 475004, China

Supporting Information

ABSTRACT: A series of novel lanthanide-containing peroxoisopolyoxomolybdates, $Na_2(NH_4)_3[H_3Ln_6(H_2O)_{26}(MoO_4)\{Mo_7O_{22}(O_2)_2\}_4]\cdot nH_2O$ [n = 24; Ln = Ce^{III} (**1**), Pr^{III} (**2**), Sm^{III} (**3**), Eu^{III} (**4**); n = 25; Ln = Nd^{III} (**5**)] and $Na_4(NH_4)_3[H_4La_5(H_2O)_{21}(MoO_4)\{Mo_7O_{22}(O_2)_2\}_4]\cdot 17H_2O$ (**6**) have successfully been synthesized by the conventional method and further characterized by elemental analyses, X-ray photoelectron spectroscopy, X-ray powder diffraction, IR and UV spectra, thermogravimetric analyses, and single-crystal X-ray diffraction. All of the six compounds are composed of the $[Ln_4(H_2O)_{16}(MoO_4)\{Mo_7O_{22}(O_2)_2\}_4]^{14-}$ polyoxoanion. **1**−**5** can further generate two-dimensional structures through Ln^{III} cations, whereas **6** shows the one-dimensional chain structure linked by La^{III} cations. These compounds represent the first examples of introducing peroxo groups into the lanthanide-containing isopolyoxomolybdates. **1** is selected as an example to investigate the electrochemical behavior of these compounds. In addition, the fluorescence analyses of **3** and **4** have been studied. The spectra exhibit obvious fluorescence signals of Sm^{III} and Eu^{III} cations.

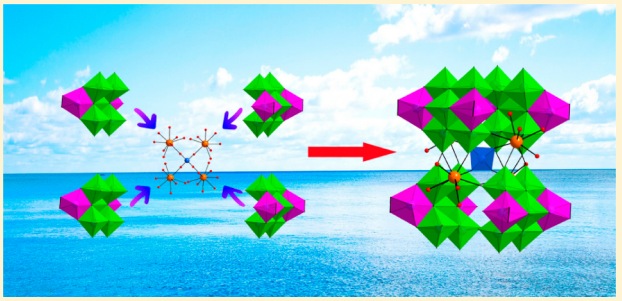

INTRODUCTION

The synthesis and exploration of polyoxometalates (POMs) have been more and more attractive during the last few decades, not only because of the enormous structural diversity but also because of the multifunctional applications in the fields of catalysis, biochemical separation, magnetism, and material science.[1−3] As we all known, oxophilic and paramagnetic lanthanide cations can impart meaningful functions, such as magnetism, luminescence, Lewis acid catalysis, and electrochemistry. In contrast to the widely used 3d metals, lanthanide ions generally adopt higher coordination sites, which are more than six. To date, numerous lanthanide-containing POMs with interesting properties have been documented.[1c,4] Furthermore, molybdenum in its high oxidation states is inclided to generate various architectures. As a result, lanthanide-containing polyoxomolybdates may merge their merits and display abundant interesting architectures with significant properties.[1c,5]

In recent years, many groups have been working on the development of lanthanide-containing polyoxomolybdates, such as Yagasaki, Müller, Krebs, Fedin, Lu, and Wang et al.[1e,4b,c,6] However, only a few structures of lanthanide cations incorporated with the heptamolybdate anion $[Mo_7O_{24}]^{6-}$ have been reported. The polyoxoanion $[Pr_4(MoO_4)(Mo_7O_{24})_4]_2^{28-}$ was reported in 1987, which represents the first example of heptamolybdate-based lanthanide derivatives.[7] The similar structures of $(NH_4)_{12}H_2[Eu_4(MoO_4)(H_2O)_{16}(Mo_7O_{24})_4]\cdot 13H_2O$ and $Na_4(NH_4)_{10}[Nd_4(MoO_4)(Mo_7O_{24})_4]\cdot 34H_2O$ were reported in 1991 and 1997, respectively.[8,9] In 2004, Krebs et al. communicated a series of lanthanide cations with the heptamolybdate anion $[Ln_4(MoO_4)(H_2O)_{16}(Mo_7O_{24})_4]^{14-}$ (Ln = La^{III}, Ce^{III}, Pr^{III}, Sm^{III}, Gd^{III}),[4b] which were isotypic with $[Eu_4(MoO_4)(H_2O)_{16}(Mo_7O_{24})_4]^{14-}$ but expanded the quantity of lanthanide cations in this type of compound. Wang's group also reported a compound $\{[(CH_3)_3N(CH_2)_2OH]_2(NH_4)_{12}\}[Ce_4(Mo_4)(H_2O)_{16}(Mo_7O_{24})_4]\cdot 8H_2O$ in 2012, which was synthesized in the choline chloride/urea eutectic mixture and without additional organic reagents.[10] In addition, there are also some reports on the introduction of peroxide groups into the polyoxomolybdates. For example, Larking et al. reported the diperoxo-heptamolybdate ion $[Mo_7O_{22}(O_2)_2]^{6-}$ in 1970.[11a] However, the combination of lanthanide cations and diperoxo-heptamolybdates (DOHMs) has not been documented until now.

POMs with dioxygen groups may have excellent catalytic properties;[11b,c] based on the considerations of the above-mentioned, we decided to use molybdates to react with lanthanide cations in the presence of peroxide with the aim of introducing peroxo groups into the system. After a great deal of experiments, six novel lanthanide-containing DOHMs, which are formulated as $Na_2(NH_4)_3[H_3Ln_6(H_2O)_{26}(MoO_4)$-

Received: April 11, 2013
Revised: June 27, 2013
Published: July 10, 2013

Table 1. Crystallographic Data and Structural Refinements for 1−6

	1	2	3	4	5	6
empirical formula	$Na_2H_{115}Ce_6Mo_{29}N_3O_{158}$	$Na_2H_{115}Pr_6Mo_{29}N_3O_{158}$	$Na_2H_{115}Sm_6Mo_{29}N_3O_{158}$	$Na_2H_{115}Eu_6Mo_{29}N_3O_{158}$	$Na_2H_{117}Nd_6Mo_{29}N_3O_{159}$	$Na_5H_{92}La_5Mo_{29}N_3O_{146}$
M_r (g mol^{-1})	6354.89	6359.63	6416.27	6425.93	6397.63	6035.17
T (K)	296(2)	296(2)	296(2)	296(2)	296(2)	296(2)
crystal system	monoclinic	monoclinic	monoclinic	monoclinic	monoclinic	monoclinic
space group	$C2/c$	$C2/c$	$C2/c$	$C2/c$	$C2/c$	$P2(1)/c$
a (Å)	37.146(2)	37.099(7)	36.7875(11)	36.688(7)	36.921(5)	17.435(12)
b (Å)	16.6971(11)	16.710(3)	16.6158(5)	16.579(4)	16.631(2)	19.441(14)
c (Å)	28.400(3)	28.416(9)	28.2367(8)	28.202(6)	28.287(4)	44.422(3)
β(deg)	123.8830(10)	123.894(2)	123.85	123.874(3)	123.872(2)	95.529(10)
volume (Å^3)	14623(2)	14622(6)	14334.2(7)	14242(5)	14421(3)	14986.7(18)
Z	4	4	4	4	4	4
D_c (Mg/m^3)	2.885	2.888	2.972	2.995	2.945	2.656
μm m^{-1}	4.352	4.484	4.992	5.193	4.68	3.851
R_{int}	0.0287	0.0407	0.0326	0.0296	0.0353	0.0323
parameters	956	956	956	956	965	1747
F(000)	11940	11964	12036	12060	12028	11128
GOF	1.094	1.067	1.047	1.02	1.069	1.060
R_1, $wR_2[I > 2\sigma(I)]$	0.0415, 0.1064	0.0372, 0.0975	0.0329, 0.0861	0.0310, 0.0821	0.0792, 0.2230	0.0473, 0.1265
R indices (all data)	0.0464, 0.1084	0.0508, 0.1030	0.0418, 0.0899	0.0368, 0.0848	0.0824, 0.2244	0.0585, 0.1315

[a] $R_1 = \Sigma||F_o| - |F_c||/\Sigma|F_o|$. [b] $wR_2 = \{\Sigma[w(F_o^2 - F_c^2)^2]/\Sigma[w(F_o^2)^2]\}^{1/2}$

$\{Mo_7O_{22}(O_2)_2\}_4]\cdot nH_2O$ [n = 24; Ln = Ce^{III} (**1**), Pr^{III} (**2**), Sm^{III} (**3**), Eu^{III} (**4**); n = 25; Ln = Nd^{III} (**5**)] and $Na_4(NH_4)_3[H_4La_5(H_2O)_{21}(MoO_4)\{Mo_7O_{22}(O_2)_2\}_4]\cdot 17H_2O$ (**6**), have been successfully synthesized and structurally characterized. The common feature of **1**−**6** is that they all consist of the isostructural polyoxoanion $\{Ln_4(H_2O)_{16}(MoO_4)[Mo_7O_{22}(O_2)_2]_4\}^{14-}$. **1**−**5** are linked by lanthanide cations to form the two-dimensional (2D) networks, whereas **6** shows the one-dimensional (1D) chain structure. To the best of our knowledge, the 1D and 2D DOHMs with lanthanide ions are reported for the first time.

EXPERIMENTAL SECTION

General Methods and Materials. All chemical reagents were purchased and used without further purification. Elemental analyses (H and N) were conducted on a Perkin-Elmer 2400-II CHNS/O analyzer. Inductively coupled plasma (ICP) analyses were performed on a Perkin-Elmer Optima 2000 ICP-OES spectrometer. The Infrared spectra (using KBr in pellets) were recorded on a Bruker VERTEX 70 IR spectrometer (4000−400 cm^{-1}). UV absorption spectra were obtained with a U-4100 spectrometer at room temperature. XPS spectra were recorded on an Axis Ultra (Kratos, U.K.) photoelectron spectroscope using monochromatic Al Kα (1486.7 eV) radiation. TG analyses were performed under a N_2 atmosphere on a Mettler−Toledo TGA/SDTA851^e instrument with the heating rate of 10 °C min^{-1} from 25 to 700 °C. X-ray powder diffraction (XRPD) was performed on a Philips X'Pert-MPD instrument with Cu Kα radiation (λ = 1.54056 Å) in the range of 2θ = 10−40 °C at 293 K. Fluorescence measurements were performed on a F-7000 fluorescence spectrophotometer. Electrochemical measurements were performed on a CS150 microcomputer-based electrochemical system (CorrTest, Wuhan, China).

Synthesis of $Na_2(NH_4)_3[H_3Ce_6(H_2O)_{26}(MoO_4)\{Mo_7O_{22}(O_2)_2\}_4]\cdot 24H_2O$ (1). $(NH_4)_6Mo_7O_{24}\cdot 4H_2O$ (0.37 g, 0.30 mmol) was dissolved in a solution consisting of 0.6 mL of ca. 30% H_2O_2 and 15 mL of H_2O. After stirring for 20 min, 1 M NaOH was added dropwise to adjust the pH to 3.3. Then, an aqueous solution (5 mL) containing $Ce(NO_3)_3\cdot 6H_2O$ (0.16 g, 0.35 mmol) was added to the above solution with stirring at room temperature. Finally, KCl (0.20 g, 2.68 mmol) was added to the resulting system. After stirring for 3 h, the solution was filtered and left to evaporate at ambient temperature. Orange crystals were afforded in three days, washed with water and air-dried. Yield: ca. 0.21 g, 57.6% [based on $Ce(NO_3)_3\cdot 6H_2O$]. Anal. Calcd (%) for $Na_2H_{115}Ce_6Mo_{29}N_3O_{158}$: H, 1.82; N, 0.66; Na, 0.72; Ce, 13.16; Mo, 43.78. Found: H, 2.04; N, 0.62; Na, 0.64; Ce, 12.89; Mo, 43.52. IR (KBr pellet): 1623 (s), 1403 (s), 929 (w), 890 (s), 844 (w), 675 (w), 630 (m), 563 (w), 472 (m), 388 (w) cm^{-1}.

Synthesis of $Na_2(NH_4)_3[H_3Pr_6(H_2O)_{26}(MoO_4)\{Mo_7O_{22}(O_2)_2\}_4]\cdot 24H_2O$ (2). The synthetic procedure was similar to that of **1**, except that $Pr(NO_3)_3\cdot 6H_2O$ (0.15 g, 0.35 mmol) was used instead of $Ce(NO_3)_3\cdot 6H_2O$. After three days, pale green block single crystals were obtained, washed with water, and air-dried. Yield: ca. 0.22 g, 59.6% [based on $Pr(NO_3)_3\cdot 6H_2O$]. Anal. Calcd (%) for $Na_2H_{115}Pr_6Mo_{29}N_3O_{158}$: H, 1.82; N, 0.66; Na, 0.72; Pr, 13.29; Mo, 43.75. Found: H, 1.98; N, 0.89; Na, 0.79; Pr, 12.86; Mo, 44.02. (KBr pellet): 1624 (s), 1545 (w), 1408 (s), 1356 (w), 893 (s), 850 (w), 681 (w), 628 (m), 561 (w), 394 (w), 478 (w) cm^{-1}.

Synthesis of $Na_2(NH_4)_3[H_3Sm_6(H_2O)_{26}(MoO_4)\{Mo_7O_{22}(O_2)_2\}_4]\cdot 24H_2O$ (3). The synthetic procedure was similar to that of **1** except that $Sm(NO_3)_3\cdot 6H_2O$ (0.15 g, 0.35 mmol) was used instead of $Ce(NO_3)_3\cdot 6H_2O$. After one week, yellow block single crystals were obtained, washed with water, and air-dried. Yield: ca. 0.15 g, 39.3% [based on $Sm(NO_3)_3\cdot 6H_2O$]. Anal. Calcd (%) for $Na_2H_{115}Sm_6Mo_{29}N_3O_{158}$: H, 1.80; N, 0.65; Na, 0.72; Sm, 14.06; Mo, 43.36. Found: H, 2.19; N, 0.59; Na, 0.68; Sm, 13.81; Mo, 43.07. IR (KBr pellet): 1623 (s), 1408 (s), 940 (w), 895 (s), 844 (w), 675 (w), 630 (m), 556 (w), 478 (m), 393 (w) cm^{-1}.

Synthesis of $Na_2(NH_4)_3[H_3Eu_6(H_2O)_{26}(MoO_4)\{Mo_7O_{22}(O_2)_2\}_4]\cdot 24H_2O$ (4). The synthetic procedure was similar to that of **1** except that $Eu(NO_3)_3\cdot 6H_2O$ (0.16 g, 0.35 mmol) was used instead of $Ce(NO_3)_3\cdot 6H_2O$. After one week, yellow block single crystals were obtained, washed with water, and air-dried. Yield: ca. 0.17 g, 45.9% [based on $Eu(NO_3)_3\cdot 6H_2O$]. Anal. Calcd (%) for $Na_2H_{115}Eu_6Mo_{29}N_3O_{158}$: H, 1.80; N, 0.65; Na, 0.72; Eu, 14.19; Mo, 43.30. Found: H, 1.97; N, 0.56; Na, 0.77; Eu, 14.32; Mo, 43.55. IR (KBr pellet): 1623 (s), 1414 (s), 940 (w), 895 (s), 850 (w), 681 (w), 630 (m), 562 (w), 472 (m), 387 (w) cm^{-1}.

Synthesis of $Na_2(NH_4)_3[H_3Nd_6(H_2O)_{26}(MoO_4)\{Mo_7O_{22}(O_2)_2\}_4]\cdot 25H_2O$ (5). The synthetic procedure was similar to that of **1**, except that $Nd(NO_3)_3\cdot nH_2O$ (0.12 g, 0.35 mmol) was used instead of $Ce(NO_3)_3\cdot 6H_2O$. After four days, kermesinus block single crystals were obtained, washed with water, and air-dried. Yield: ca. 0.18 g, 48.6% [based on $Nd(NO_3)_3\cdot nH_2O$]. Anal. Calcd (%) for

dx.doi.org/10.1021/cg400536e | Cryst. Growth Des. 2013, 13, 3554−3560

$Na_2H_{117}Nd_6Mo_{29}N_3O_{159}$: H, 1.84; N, 0.66; Na, 0.72; Nd, 13.53; Mo, 43.49. Found: H, 2.02; N, 0.61; Na, 0.62; Nd, 13.27; Mo, 43.18. IR (KBr pellet): 1624 (s), 1403 (s), 940 (w), 895 (s), 850 (w), 675 (w), 624 (m), 560 (w), 478 (m), 382 (w) cm^{-1}.

Synthesis of $Na_4(NH_4)_3[H_4La_5(H_2O)_{21}(MoO_4)\{Mo_7O_{22}(O_2)_2\}_4]\cdot 17H_2O$ (6). The synthetic procedure was similar to that of **1** except that $LaCl_3\cdot nH_2O$ (0.09 g, 0.35 mmol) was used instead of $Ce(NO_3)_3\cdot 6H_2O$. After one week, yellow block single crystals were obtained, washed with water, and air-dried. Yield: ca. 0.19 g, 45.0% (based on $LaCl_3\cdot nH_2O$). Anal. Calcd (%) for $Na_5H_{92}La_5Mo_{29}N_3O_{146}$: H, 1.52; N, 0.70; Na, 0.76; La, 11.51; Mo, 46.10. Found: H, 1.77; N, 0.74; Na, 0.82; La, 11.79; Mo, 46.26. IR (KBr pellet): 1624 (s), 1412 (s), 897 (s), 843 (w), 679 (w), 629 (m), 558 (w), 476 (m), 383 (w) cm^{-1}.

X-ray Crystallographic Analyses. Single crystals for X-ray structure analysis were performed on Bruker CCD Apex-II diffractometer with Mo Kα radiation (λ = 0.71073 Å) at 296 K. Routine Lorentz polarization and empirical absorption corrections were applied. The structures of compounds **1**−**6** were solved by direct methods refined by full-matrix least-squares refinements on F^2 using SHELXL-97, and an absorption correction was performed using the SADABS program. No hydrogen atoms associated with the water molecules were located from the difference Fourier map. The hydrogens of all the nitrogen atoms were added in calculated positions and were refined isotropically as a riding mode by the default SHELXL parameters. NH_4^+ and lattice H_2O could not be distinguished based on electron densities, and we thus determine the lattice water molecules and NH_4^+ ions by elemental analyses. A summary of crystallographic date and structural refinements for **1**−**6** is given in Table 1. Further details on the crystal structure investigation may be obtained from the Fachinformationszentrum Karlsruhe, 76344 Eggenstein-Leopoldshafen, Germany [fax: (+49)7247−808−666; e-mail: crysdata@fiz-karlsruhe.de], on quoting the depository numbers CSD-425719 (**1**), CSD-425720 (**2**), CSD-425721 (**3**), CSD-425722 (**4**), CSD-425723 (**5**), and CSD-425724 (**6**), respectively.

RESULTS AND DISCUSSION

Syntheses. To date, lanthanide-containing polyoxomolybdates are well-developed.[1e,4b,c,6] However, there still remains much research on lanthanide cations with DOHMs to be explored, especially the syntheses of high-dimensional structures, which have attracted our great interest. In this paper, we chose heptamolybdate, as a building block and synthesized six compounds with 1D and 2D structures. Compounds **1**−**6** were synthesized in the aqueous solution by the reaction of $(NH_4)_6Mo_7O_{24}\cdot 4H_2O$ with Ln^{III} cations in the presence of H_2O_2 by adjusting the pH to ca. 3.3 with 1 M NaOH under ambient temperature. Parallel experiments show that several factors affect the formation and the quality of the crystals: (a) In the process of synthesis, the pH value plays an important role in isolating the six compounds and should be carefully controlled between 2.9 and 3.5. When the pH value is lower than 2.9 or higher than 3.5, there are a large number of precipitates in the course of crystallization. (b) The best ratio of $[Mo_7O_{24}]^{6-}/Ln^{3+}$ is 6/7, when the ratio varies from 6/7 to 3/1 under the same conditions, we can also obtain the crystals of **1**−**6** but with poor quality and low yield. (c) The source of molybdenum in the reactions is preferably $(NH_4)_6Mo_7O_{24}\cdot 4H_2O$. If it is replaced by other molybdenum sources such as Na_2MoO_4, only some amorphous precipitates are obtained. Finally, the optimum conditions are listed in Experimental Section. To investigate the effect of different lanthanide cations on structural diversity, we have changed the heavy lanthanide ions such as Tb^{III}, Dy^{III}, or Ho^{III} to La^{III}, Ce^{III}, Pr^{III}, Nd^{III}, Sm^{III}, or Eu^{III} ions under the same conditions; unfortunately, only some amorphous precipitates are obtained, which indicates that heavy lanthanide ions may have low activity in this reaction system.

Structural Descriptions. Single-crystal X-ray diffraction analyses reveal that the compounds **1**−**5** crystallize in the monoclinic $C2/c$ space group, and **6** crystallizes in the monoclinic $P2(1)/c$ space group. Bond valence sum (BVS) calculations[12] indicate that all Mo and Ln atoms are in +6 and +3 oxidation states, respectively. In consideration of the charge balance, some protons, which are regarded as the average bond valence sums of O atoms, need to be added. All six compounds are isostructural and contain the same polyoxoanion $[Ln_4(H_2O)_{16}(MoO_4)\{Mo_7O_{22}(O_2)_2\}_4]^{14-}$, hence, only the structure of **1** is taken as an example to describe in detail.

Compound **1** consists of the polyoxoanion $[Ce_6(H_2O)_{26}(MoO_4)\{Mo_7O_{22}(O_2)_2\}_4]^{8-}$, two isolated Na^+ ions, three NH_4^+ cations, twenty-four lattice water molecules, and three protons based on the charge balance (Figure1a). The

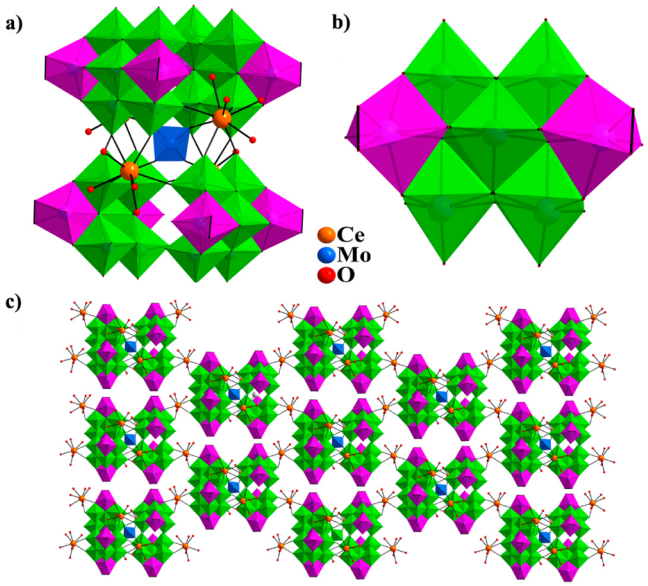

Figure 1. (a) Polyhedral/ball-and-stick representation of polyoxoanion in **1**. (b) Polyhedral representation of $[Mo_7O_{22}(O_2)_2]^{6-}$ unit. (c) 2D layer of **1**; color codes: MoO_6, green; MoO_7, purple red; MoO_4, blue. H^+, Na^+, and NH_4^+ cations are omitted.

unit cell views of **1** are shown in Figure S1 of the Supporting Information. The polyoxoanion $[Ce_6(H_2O)_{26}(MoO_4)\{Mo_7O_{22}(O_2)_2\}_4]^{8-}$ can be considered as the assembly of four fused $[Ce(H_2O)_4\{Mo_7O_{22}(O_2)_2\}]^{3-}$ monomers encapsulating a central tetrahedral MoO_4 group, each $[Mo_7O_{22}(O_2)_2]^{6-}$ unit connects one $[Ce(H_2O)_5]^{3+}$ cation to form the 2D layer (Figure 1c). In compound **6**, $\{La_4(H_2O)_{16}(MoO_4)[Mo_7O_{22}(O_2)_2]_4\}^{14-}$ is connected by $La^{III}(5)$ to form the 1D structure (Figure 2), that is the exclusive difference between **6** and **1**−**5**, which may be attributed to the larger radius of the La^{III} cation compared to the other Ln^{III} cations. The unit cell views of the structure of **6** are shown in Figure S2 of the Supporting Information. In the MoO_4 group, the Mo−O distances are in the range of 1.759(4)−1.766(5) Å, and O−Mo−O angles are in the range of 108.5(3)−110.2(4)°. Each oxygen atom of the central MoO_4 unit is bonded to one cerium atom. All four cerium atoms show nine-coordinated tricapped trigonal prismatic geometry, defined by one oxygen atom from the central MoO_4 unit, four oxygen atoms from three different

dx.doi.org/10.1021/cg400536e | Cryst. Growth Des. 2013, 13, 3554−3560

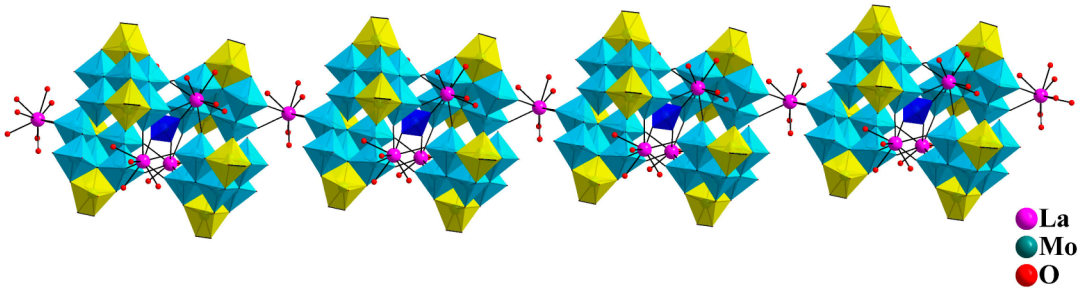

Figure 2. 1D Chain structure of **6**. Color codes: MoO_6, light blue; MoO_7, yellow; and MoO_4, dark blue. H^+, Na^+, and NH_4^+ cations are omitted.

$[Mo_7O_{22}(O_2)_2]^{6-}$ units, and four oxygen atoms from four water molecules (Figure 3a). The assembly of the structure is

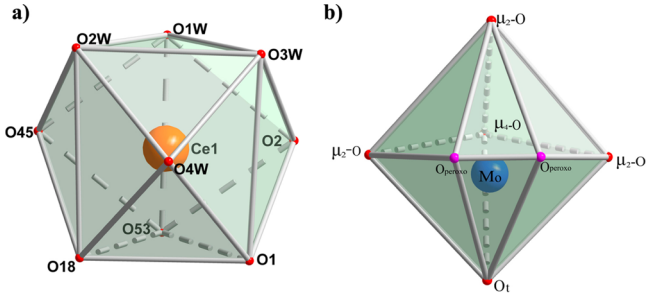

Figure 3. The coordination environments of (a) Ce1 and (b) Mo2.

Scheme 1. Coordination Mode of the Polyoxoanion of 1

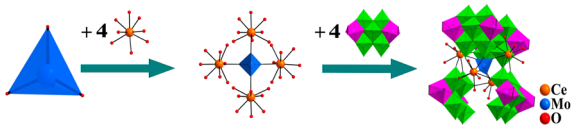

illustrated in Scheme 1. In the coordination configuration of the $Ce^{III}(1)$ cation, the O1W, O2W, O3W group and the O1, O18, O53 group dihedral angle for the two bottom planes constituted 4.04°, and the distances of the $Ce^{III}(1)$ cation and the two bottom planes are 1.775 and 1.752 Å, respectively. The O2W, O18, O1W, O53 group, the O1W, O53, O3W, O1 group, and the O2W, O18, O3W, O1 group form the three side planes of the trigonal prism, and their standard deviations from their least squares are 0.143, 0.047, and 0.103 Å, respectively. The distances between the Ce^{III} (1) cation and the three side planes are 0.850, 0.877, 0.932 Å, respectively. In addition, the O45, O2, and O4W occupy the three cap positions covering the side planes, defined by the O2W, O18, O1W, O53 group, the O1W, O53, O3W, O1 group, and the O2W, O18, O3W, O1 group, respectively. The distances between the three cap positions and the three planes are 1.668, 1.634, and 1.690 Å, respectively. The above-mentioned data indicate that the tricapped trigonal prism is somewhat distorted. The selected bond lengths and bond angles of the central $\{Ln_4(H_2O)_{16}(MoO_4)\}^{10+}$ unit are given in Tables S1 and S2 of the Supporting Information. All the lanthanide ions are coordinated by oxygen atoms in a similar way.

The $[Mo_7O_{22}(O_2)_2]^{6-}$ unit is composed of five MoO_6 octahedron and two MoO_7 pentagonal bipyramids through sharing edges and corners (Figure1b). It is evident that the DOHMs in this work have the same general appearance as the normal heptamolybdate, but the difference is that two peroxo groups replace two oxygen atoms located at the terminal of each heptamolybdate. The two Mo atoms coordinated to the peroxo groups are ligated by three double-bridged O atoms, one quadruply bridged O atom, one terminal O atom, and one terminal η^2-coordinated peroxo unit to define a distorted pentagonal bipyramidal coordination polyhedron (Figure 3b). The other five Mo atoms remain the conventional MoO_6 polyhedra. The Mo−O bond lengths in each subunit adjacent to the peroxo groups (O8−O9, O22−O23, O34−O35, and O48−O49, respectively) are in the range of 1.906(8)−1.932(9) Å, and the peroxide O−O bond lengths are 1.359(13) to 1.398(13) Å, respectively. Each $[Mo_7O_{22}(O_2)_2]^{6-}$ unit can be regarded as a tetradentate ligand bonded to three Ce^{III} cations. Two of the five MoO_6 octahedron of the $[Mo_7O_{22}(O_2)_2]^{6-}$ unit provide two terminal oxygen atoms for the Ce−O bonds. Compared with the similar compounds which are mentioned above, such as $[Pr_4(MoO_4)(Mo_7O_{24})_4]_2^{28-}$,[7] our compounds not only introduce O_2^{2-} anions into the system but also are extended to a multidimensional structure.

FT−IR and XRPD Patterns. The peak shapes of the IR spectra in the 400−1000 cm^{-1} region of **1**−**6** are similar (Figures S3 and S4 of the Supporting Information), indicating the polyoxoanions in **1**−**6** are isostructures. The band located at around 845 cm^{-1} is assigned to the peroxo group ν(O−O) vibration,[13a] while the characteristic peaks in the ranges of 940−890 cm^{-1} and 685−470 cm^{-1} are attributed to ν(Mo═O) and ν(Mo−O−Mo) vibrations, respectively.[13b] The XRPD patterns for compounds **1**−**6** are presented in Figure S5 and S6 of the Supporting Information. The diffraction peaks of both simulated and experimental patterns well match with each other, which indicates the phase purities of compounds **1**−**6**.

XPS Spectra. As for **1** (Figure 4), XPS spectrum for cerium center exhibits two peaks at 881.8 and 884.9 eV corresponding to Ce^{III} ($3d_{5/2}$), while two other peaks are exhibited at 902.9 and 904.2 eV, corresponding to Ce^{III} ($3d_{3/2}$).[10] The spectrum for the molybdenum center shows two peaks at 231.5 and 234.5 eV, corresponding to Mo^{VI} ($3d_{5/2}$) and Mo^{VI} ($3d_{3/2}$), respectively.[10] For **6**, the XPS spectrum exhibit two peaks at 284.1 and 237.9 eV, which are ascribed to La^{III} ($3d_{5/2}$), and two other peaks at 851.1 and 854.7 eV, which are ascribed to La^{III} ($3d_{3/2}$). Two peaks at 231.6 and 234.6 eV are corresponding to Mo^{VI} ($3d_{5/2}$) and Mo^{VI} ($3d_{3/2}$), respectively (Figure S7 of the Supporting Information).[14]

Thermogravimetric (TG) Analyses. Since complexes **1**−**6** display two types of structures, **1** and **6** are chosen for thermogravimetric analyses in the temperature range of 25−700 °C. The TG curve of **1** exhibits one slow step of weight loss (Figure S8 of the Supporting Information), giving a total loss of 18.56% (calcd 19.42%) in the range of 25−450 °C. The

dx.doi.org/10.1021/cg400536e | Cryst. Growth Des. 2013, 13, 3554−3560

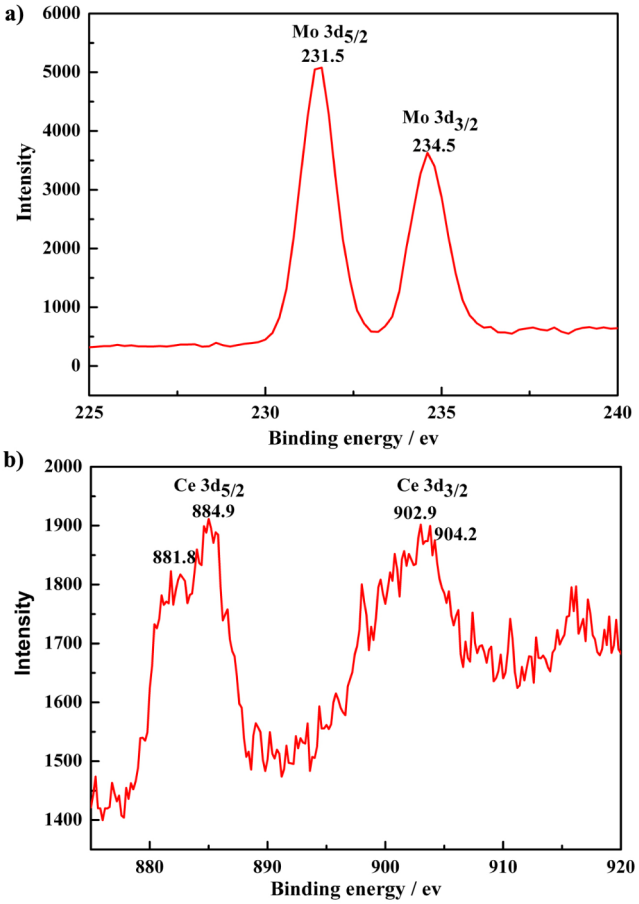

Figure 4. (a) XPS spectra of **1** for Mo $3d_{5/2}$ and Mo $3d_{3/2}$. (b) XPS spectra of **1** for Ce $3d_{5/2}$ and Ce $3d_{3/2}$.

total weight loss can be assigned to 24 crystal water molecules, 26 coordinated water molecules, the dehydration of three protons, three NH_3 molecules, and eight O_2 molecules. The TG curve of **6** also shows one slow step of weight loss (Figure S9 of the Supporting Information), and the curve giving a total loss of 16.25% (calcd 17.01%) in the range of 25−700 °C, which can be attributed to the release of 17 crystal water molecules, 21 coordinated water molecules, the dehydration of 4 protons, 3 NH_3 molecules, and 8 O_2 molecules.

UV Spectra. All the UV spectra of compounds **1**−**6** in aqueous solution display two similar absorption bands centered at 205−207 nm and 231−233 nm (Figures S10 and S11 of the Supporting Information). The higher energy band can be assigned to the charge transfer transitions of the $O_t \rightarrow$ Mo band, whereas the lower one can be attributed to those of the $O_{b,c} \rightarrow$ Mo band, suggesting the presence of polyoxoanions.[15] In order to investigate the stability of **1** in solution, the in situ spectroscopic measurements were performed in the aqueous system (Figure 5). The absorption band at 207 nm is not changed, while the absorbance becomes a little stronger than that at the initial state until at 16 h. The consequence reveals that the aqueous system of **1** can stably exist at least 16 h at ambient temperature.

It is well-known that the POMs are commonly sensitive to the pH value of the studied media. Therefore, in order to investigate the influences of the pH values on the stability of compounds in aqueous solution, compound **1** has also been elaborately probed by means of UV spectra. Diluted HCl and

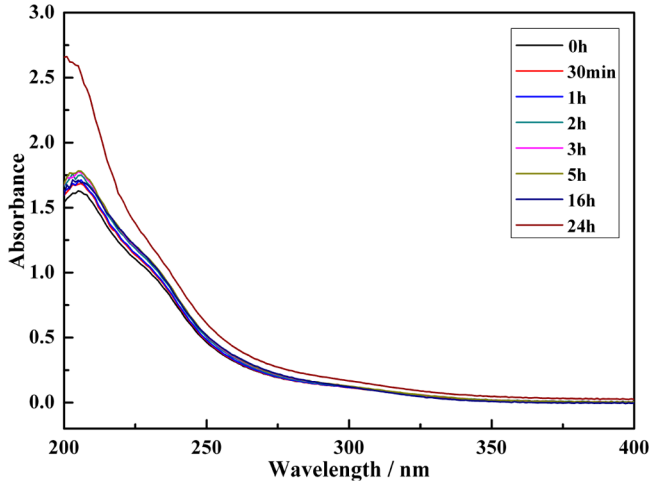

Figure 5. The influence of time on the stability of **1** in the aqueous solution.

NaOH solution were used to adjust the pH values in the acidic direction and in the alkaline direction, respectively. The pH value of **1** in water (5×10^{-5} mol/L^{-1}) was 4.2. As is shown in Figure 6a, the UV spectra of **1** in aqueous solution display two absorption bands at 207 and 233 nm; when the pH value gradually decreases to 3.7, the absorbance band at 207 nm occurred red-shifted but not obvious. With further decrease in the pH value, the absorbance band at 207 nm is gradually red-shifted, while the other absorbance band at 233 nm slowly disappears. The reason for the red-shift of the $O_t \rightarrow$ Mo band may be related to the protonation of the terminal oxygen atoms of polyoxoanions.[15,16] In contrast, when the pH value of **1** increases (Figure 6b), the absorption band at 207 nm is weaker and weaker until it vanishes. However, the solution absorbance becomes larger, suggesting the decomposition of the skeleton. The results indicate that compound **1** has been decomposed at a pH lower than 3.7 and higher than 10.2; that is to say, **1** can remain stable in a large pH range.

Cyclic Voltammetry. To explore the electrochemical property of **1**, cyclic voltammetric (CV) measurements of the compound were recorded in the pH = 3.3 (0.2 M H_2SO_4 + Na_2SO_4) buffer solution at a scan rate of 100 mV s^{-1} (Figure S12 of the Supporting Information). Two reversible redox peaks appear in the potential range from −600 to 1400 mV versus SCE, and the two reversible reductions at $E_{1/2} = (E_{pa} + E_{pc})/2$ = 48.5 and 828 mV over the course of the cathodic sweep. The two redox peaks could be ascribed to Mo^{VI}/Mo^{V}.[10]

Fluorescence Spectroscopy. The solid-state fluorescence properties of **3** and **4** have been investigated at room temperature. The emission spectrum of **3** at the excited wavelength of 435 nm exhibits the characteristic emission of Sm^{III}. Three characteristic bands can be observed (Figure 7a), which are attributed to $^4G_{5/2} \rightarrow {}^6H_{5/2}$ (551 nm), $^4G_{5/2} \rightarrow {}^6H_{7/2}$ (570 nm), and $^4G_{5/2} \rightarrow {}^6H_{9/2}$ (653 nm) transitions, respectively.[17] **4** exhibits intense photoluminescence upon excitation at 394 nm, consisting of the typical Eu^{III} fluorescence emission. The six characteristic emission bands at 536, 557, 593, 615, 652, and 703 nm are shown in Figure 7b, attributing to the $^5D_1 \rightarrow {}^7F_1$, $^5D_1 \rightarrow {}^7F_2$, $^5D_0 \rightarrow {}^7F_1$, $^5D_0 \rightarrow {}^7F_2$, $^5D_0 \rightarrow {}^7F_3$, and $^5D_0 \rightarrow {}^7F_4$ transitions, respectively.[18a] To the best of our knowledge, the $^5D_0 \rightarrow {}^7F_1$ (593 nm) transition belongs to a magnetic dipole transition, and its intensity is different from the crystal field strength acting on the Eu^{III} cation, whereas the $^5D_0$

dx.doi.org/10.1021/cg400536e | Cryst. Growth Des. 2013, 13, 3554−3560

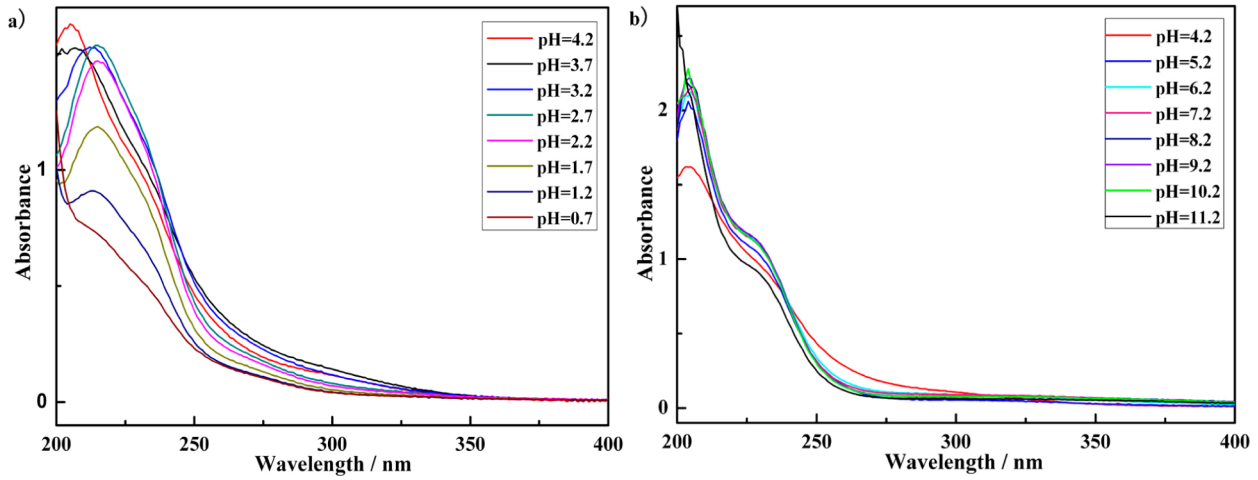

Figure 6. Influence of the pH values on the stability of **1** in aqueous solution: (a) The UV spectral evolution in the acidic direction. (b) The UV spectral evolution in the alkaline direction.

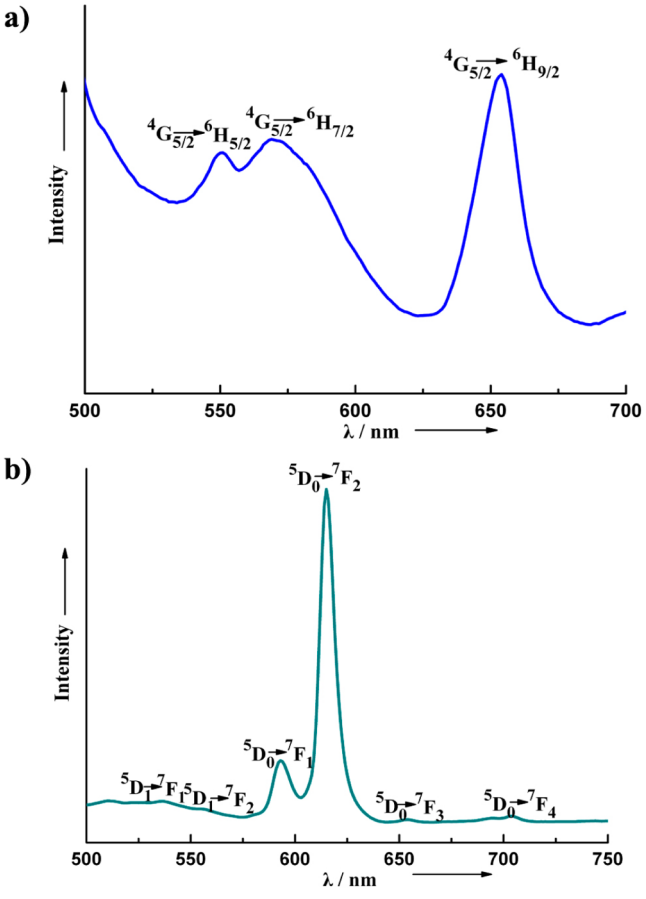

Figure 7. Solid-state emission spectra of compounds (a) **3** and (b) **4** at room temperature.

$\rightarrow {}^7F_2$ (615 nm) transition induced by the electric dipole moment is extremely sensitive to chemical bonds in the vicinity of the Eu^{III} cation.[18b] In accordance with the Judd–Ofelt theory, the magnetic dipole transition is permitted, while the electric dipole transition is forbidden; that is to say, the intensity of the electric dipole is stronger than that of the magnetic dipole, which indicates that the coordination environment of the Eu^{III} cation is asymmetric, confirmed by crystallographic analyses.[17,18]

CONCLUSIONS

In summary, six novel lanthanide-containing DOHMs have been obtained by the conventional method and structurally characterized by elemental analyses, ICP, XRPD, CV, IR and UV–vis spectra, TG analyses, and single-crystal X-ray diffraction. The six polyoxoanions consist of four $[Mo_7O_{22}(O_2)_2]^{6-}$ building blocks encapsulating the $\{Ln_4(H_2O)_{16}(MoO_4)\}^{10+}$ core, of which **1**–**5** can further generate 2D networks and **6** can generate a 1D chain structure. The six compounds represent the first examples of introducing peroxo groups into the lanthanide-stabilized isopolymolybdate system, which enriches various geometric structures and potential properties in the family of lanthanide-substituted isopolymolybdates.

ASSOCIATED CONTENT

Supporting Information

Crystallographic data of **1**–**6** in CIF format. Bond lengths and bond angles of compound **1**–**6**, bond valence sum calculations of all the oxygen atoms for **1**, and representations of XPRD spectra, IR spectra, UV spectra of **1**–**6**, XPS spectra of **6**, cycle voltammograms of **1**, and TG curves of **1** and **6**. This material is available free of charge via the Internet at http://pubs.acs.org.

AUTHOR INFORMATION

Corresponding Author

*J.N.: e-mail, jyniu@henu.edu.cn. J.W.: e-mail, jpwang@henu.edu.cn; tel, (+86) 378 3886876; fax, (+86) 378 3886876.

Notes

The authors declare no competing financial interest.

ACKNOWLEDGMENTS

The authors thank the National Natural Science Foundation of China, the Foundation of Education Department of the Henan Province, and the Natural Science Foundation of the Henan Province for financial support.

REFERENCES

(1) (a) Long, D. L.; Tsunashima, R.; Cronin, L. *Angew. Chem., Int. Ed.* **2010**, *49*, 1736–1758. (b) Cadot, E.; Sokolov, M. N.; Fedin, V. P.; Simonnet-Jégat, C.; Floquet, S.; Sécheresse, F. *Chem. Soc. Rev.* **2012**, *41*, 7335–7353. (c) Zhang, S. W.; Wang, K.; Zhang, D. D.; Ma, P. T.;

Niu, J. Y.; Wang, J. P. *CrystEngComm* **2012**, *14*, 8677−8683. (d) Niu, J. Y.; Zhang, S. W.; Chen, H. N.; Zhao, J. W.; Ma, P. T.; Wang, J. P. *Cryst. Growth Des.* **2011**, *11*, 3769−3777. (e) Wang, X. L.; Guo, Y. Q.; Li, Y. G.; Wang, E. B.; Hu, C. W.; Hu, N. H. *Inorg. Chem.* **2003**, *42*, 4135−4140. (f) Katsoulis, D. E. *Chem. Rev.* **1998**, *98*, 359−388.

(2) (a) Song, Y. F.; Tsunashima, R. *Chem. Soc. Rev.* **2012**, *41*, 7384−7402. (b) Oms, O.; Dolbecq, A.; Mialane, P. *Chem. Soc. Rev.* **2012**, *41*, 7497−7536. (c) Mizuno, N.; Misono, M. *Chem. Rev.* **1998**, *98*, 199−218. (d) Dolbecq, A.; Dumas, E.; Mayer, C. R.; Mialane, P. *Chem. Rev.* **2010**, *110*, 6009−6048. (e) Kortz, U.; Müller, A.; Slageren, J. V.; Schnack, J.; Dalal, N. S.; Dressel, M. *Coord. Chem. Rev.* **2009**, *253*, 2315−2327.

(3) (a) Izarova, N. V.; Pope, M. T.; Kortz, U. *Angew. Chem., Int. Ed.* **2012**, *51*, 9492−9510. (b) Bassil, B. S.; Dickman, M. H.; Römer, I.; Kammer, B. V. D.; Kortz, U. *Angew. Chem., Int. Ed.* **2007**, *46*, 6192−6195. (c) Müller, A.; Roy, S. *Coord. Chem. Rev.* **2003**, *245*, 153−166.

(4) (a) Yamase, T. *Chem. Rev.* **1998**, *98*, 307−326. (b) Burgemeister, K.; Drewes, D.; Limanski, E. M.; Küper, I.; Krebs, B. *Eur. J. Inorg. Chem.* **2004**, *13*, 2690−2694. (c) Izarova, N. V.; Sokolov, M. N.; Samsonenko, D. G.; Rothenberger, A.; Naumov, D. Y.; Fenske, D.; Fedin, V. P. *Eur. J. Inorg. Chem.* **2005**, *24*, 4985−4996. (d) Cronin, L.; Beugholt, C.; Krickemeyer, E.; Schmidtmann, M.; Bögge, H.; Kögerler, P.; Luong, T. K. K.; Müller, A. *Angew. Chem., Int. Ed.* **2002**, *41*, 2805−2808. (e) Kido, J.; Okamoto, Y. *Chem. Rev.* **2002**, *102*, 2357−2368. (f) Wassermann, K.; Pope, M. T. *Inorg. Chem.* **2001**, *40*, 2763−2768.

(5) (a) Lacorre, P.; Goutenoire, F.; Bohnke, O.; Retoux, R.; Laligant, Y. *Nature* **2000**, *404*, 856−858. (b) Lü, J.; Shen, E. H.; Li, Y. G.; Xiao, D. R.; Wang, E. B.; Xu, L. *Cryst. Growth Des.* **2005**, *5*, 65−67.

(6) (a) Kitamura, A.; Ozeki, T.; Yagasaki, T. *Inorg. Chem.* **1997**, *36*, 4275−4279. (b) Müller, A.; Beugholt, C.; Bögge, H.; Schmidtmann, M. *Inorg. Chem.* **2000**, *39*, 3112−3113.

(7) Fedosseev, A. M.; Grigorév, M. S.; Yanovskii, A. I.; Struchkovyn, T.; Spitsin, V. I. *Doklady Academii Nauk SSSR* **1987**, 111−114.

(8) Naruke, B. H.; Ozeki, T.; Yagasaki, T. *Acta Crystallogr.* **1991**, *C47*, 489−492.

(9) Cai, X. Z.; Wang, S. M.; Huang, J. F.; Guan, H. M.; Lin, X. *Chin. J. Struct. Chem.* **1997**, *16*, 328−334.

(10) Liu, L.; Wang, S. M.; Chen, W. L.; Lu, Y.; Li, Y. G.; Wang, E. B. *Inorg. Chem. Commun.* **2012**, *23*, 14−16.

(11) (a) Stomberg, R.; Trysberg, L.; Larking, I. *Acta Chem. Scand.* **1970**, *24*, 2678−2679. (b) Aubry, C.; Chottard, G.; Platzer, N.; Brégeault, J. M.; Thouvenot, R.; Chauveau, F.; Huet, C.; Ledon, H. *Inorg. Chem.* **1991**, *30*, 4409−4415. (c) Duncan, D. C.; Chambers, R. C.; Hecht, E.; Hill, C. L. *J. Am. Chem. Soc.* **1995**, *117*, 681−691.

(12) Brown, I. D.; Altermatt, D. *Acta Crystallogr.* **1985**, *B41*, 244−247.

(13) (a) Piquemal, J. Y.; Salles, L.; Chottard, G.; Herson, P.; Ahcine, C.; Brégeault, J. M. *Eur. J. Inorg. Chem.* **2006**, 939−947. (b) Coué, V.; Dessapt, R.; Bujoli-Doeuff, M.; Evain, M.; Jobic, S. *Inorg. Chem.* **2007**, *46*, 2824−2835.

(14) Serrano-Lotina, A.; Martin, A. J.; Folgado, M. A.; Daza, L. *Int. J. Hydrogen. Energy* **2012**, *37*, 12342−12350.

(15) Li, S. Z.; Zhao, J. W.; Ma, P. T.; Du, J.; Niu, J. Y.; Wang, J. P. *Inorg. Chem.* **2009**, *48*, 9819−9830.

(16) Li, S. Z.; Guo, Y. Y.; Zhang, D. D.; Ma, P. T.; Qiu, X. Y.; Wang, J. P.; Niu, J. Y. *Dalton Trans.* **2012**, *41*, 5235−5240.

(17) Niu, J. Y.; Zhang, X. Q.; Yang, D. H.; Zhao, J. W.; Ma, P. T.; Kortz, U.; Wang, J. P. *Chem.—Eur. J.* **2012**, *18*, 6759−6762.

(18) (a) Xia, J.; Zhao, B.; Wang, H. S.; Shi, W.; Ma, Y.; Song, H. B.; Cheng, P.; Liao, D. Z.; Yan, S. P. *Inorg. Chem.* **2007**, *46*, 3450−3458. (b) Wang, X. L.; Guo, Y. Q.; Li, Y. G.; Wang, E. B.; Hu, C. W.; Hu, N. H. *Inorg. Chem.* **2003**, *42*, 4135−4140.